EPSC2018

EXO4/TP14/OPS9/MD6 abstracts

EPSC Abstracts
Vol. 12, EPSC2018-276, 2018
European Planetary Science Congress 2018

Towards a new tool for modelling non-adiabatic giant planets

Ludwig Scheibe, Nadine Nettelman and Ronald Redmer
Institute for Physics, University of Rostock, Germany

Abstract

We present work in progress towards a modelling approach for the interior and evolution of giant planets. It follows the well-known method by Henyey et al. (1964) [1] for stars. In contrast to conventional modelling assumptions for Jupiter and Saturn [2] and Uranus and Neptune [3], our goal is to go beyond the premise of adiabatic interiors, as the presence of stably stratified and thus non-adiabatic regions is indicated by some magnetic field models for the ice giants [4]. Therefore, we solve self-consistently for the local temperature gradient, the compositional gradient and the heat flux, accounting for heat and particle transport by convection and diffusion. This way we hope to gain new insight into the origin of the low intrinsic luminosity of Uranus and the high intrinsic luminosity of Neptune. Here, we present the theoretical foundations and implementation of the model as well as first results.

Acknowledgements

This project was funded by the DFG grant NN1734/2 within the DFG research unit FOR 2440 “Matter Under Planetary Interior Conditions”.

References

[1] Henyey, L.G., Forbes, J.E., and Gould, N.L.: A New Method of Automatic Computation of Stellar Evolution. ApJ, Vol. 139, pp. 306-317, 1964.

[2] Guillot, T.: A comparison of the interiors of Jupiter and Saturn. Planet. Space Sci., Vol. 47, pp. 1183-1200, 1999.

[3] Nettelmann, N., Helled, R., Fortney, J.J., and Redmer, R.: New indication for a dichotomy in the interior structure of Uranus and Neptune from the application of modified shape and rotation data. Planet. Space Sci., Vol. 77, pp. 143-151, 2013.

[4] Stanley, S. and Bloxham, J.: Convective-region geometry as the cause of Uranus’ and Neptune’s unusual magnetic fields. Nature, Vol. 428, pp. 151-152, 2004.

EPSC Abstracts
Vol. 12, EPSC2018-310, 2018
European Planetary Science Congress 2018

Measurability of the fluid Love number k_2 in WASP-121b

Hugo Hellard (1), Szilárd Csizmadia (1), Sebastiano Padovan (1), Frank Sohl (1), Doris Breuer (1), Tilman Spohn (1), and Heike Rauer (1,2)
(1) Institute of Planetary Research, German Aerospace Centre, Berlin, Germany, (2) Institute of Geological Sciences, Free University, Berlin, Germany (hugo.hellard@dlr.de)

Abstract

We are witness to a great and increasing interest in internal structure, composition and evolution of exoplanets. However, direct measurements of exoplanetary mass and radius are insufficient to distinguish between different internal structure and composition models–known as the mass-radius degeneracy– justifying the need for an additional observable [6]. As already introduced in the litterature [1, 2], we show that planetary surface deformations coming from tidal and rotational effects cause distortions in the transit curves. These distortions can be expressed through the fluid Love numbers k_j, providing additional information on the planetary internal structure [3]. We discuss detectability of non-sphericity effects in transit curves of WASP-121b in the light of dedicated space missions (*e.g.* Kepler, TESS, JWST, PLATO).

1. Introduction

Close-in objects with typical orbital periods shorter than ten days undergo strong rotational and tidal distortions, modifying their shape from spherical to more complicated ones. We assume both components in hydrostatic equilibrium, hence behaving as a fluid, critical to interpret the shape in terms of internal structure. The surficial deformations depend on the body's internal structure, and may be expressed through the fluid Love numbers k_j [4, 5] (section 2). In particular, the second-degree Love number k_2 tells us how much mass is concentrated towards the component's centre. As a result of these deformations, the stellar eclipsed area or planetary reflecting area will differ, changing the corresponding transit curves (section 3).

2. Model

The perturbing potential arises from the centrifugal force due to the planet's self rotation and from the tidal force coming from its host star. One may assume a tilted spin axis w.r.t. the orbital plane. By expressing the perturbing potential in spherical harmonics, Love (1911) and Kopal (1959) [5, 4] showed that the surface radius is given by

$$r(\theta,\phi) = R_p\left(1 + q\sum_{j=2}^{4} h_{j,p} P_j(\lambda)\left(\frac{R_p}{d}\right)^{j+1} - \frac{1}{3}(1+q)h_{2,p}F_p^2\left(\frac{R_p}{d}\right)^3 P_2(\cos(\Theta))\right) \quad (1)$$

where θ is the co-latitude, ϕ is the longitude, R_p is the planetary mean radius, $q = \frac{m_s}{m_p}$ is the mass ratio, P_j is the Legendre polynome of degree j, d is the orbital distance, $F_p = \frac{\omega_{rot}}{\omega_{orb}}$ is the planetary angular rotation ratio. λ and Θ are angles which depend on θ, ϕ, and on the tilted angle of the spin axis, and $h_{j,p} = 1 + k_{j,p}$ are the planetary fluid Love numbers. A value of $h_2 = 1$ means the mass is concentrated at the body's centre (mass-point model), while $h_2 = 2.5$ is reached for a fully homogeneous body. A similar expression can be found for the stellar surface deformations through an obvious interchange of signs.
We assume synchronously locked orbits, *i.e.* $F_p = F_s = 1$, with a non-tilted spin axis, *i.e.* $\Theta = \theta$. For the star, the mass-point model is a good approximation, *i.e.* $h_{j,s} = 1$. Hence, depending on the planetary internal structure (enclosed in $h_{j,p}$), the planet's resulting projected shape onto the plane-of-sky will differ, leading to different photometric curves.
We compute transit curves for WASP-121b, for different values of $h_{2,p}$ and keeping $h_{3,p} = h_{4,p} = 1$.

3. Results

In Figure 1 we present a single transit event for $h_2 = 1.3$, and its best spherical fit. One may recognize the highest distoritions in the ingress and egress phases of the transit. The maximum distortion amounts to roughly 900 ppm. This is explained by the fact that WASP-121b orbits close to its Roche limit (at roughly

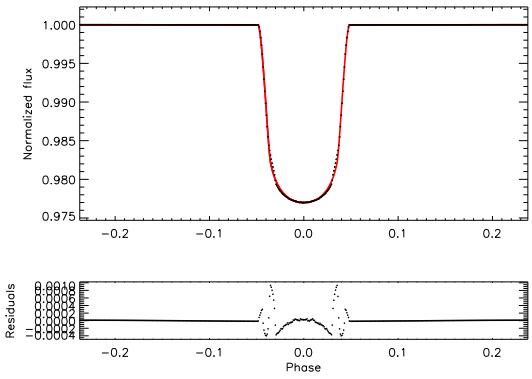

Figure 1: Upper panel: single transit event of WASP-121b for $h_2 = 1.3$ (black dots), and its best spherical fit (red line). Lower panel: residuals (distorted - spherical).

twice its Roche limit), and thus is subjected to huge tidal deformations. Figure 2 presents the expected signal-to-noise ratio (S/N) of this effect, as a function of h_2 (*i.e.* internal structure). The noise levels have been computed for a composite light curve from 10 observed transits, binned into 2 minute intervals. With the exception of TESS, we show that PLATO,

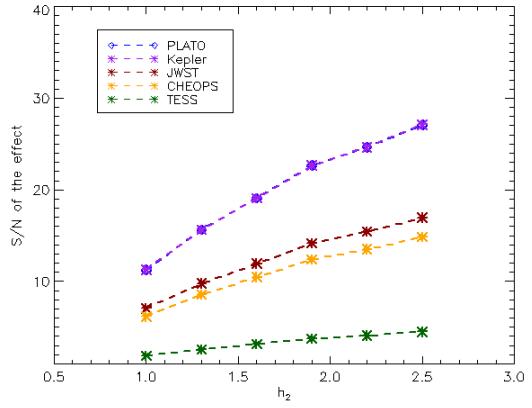

Figure 2: S/N of the distortions as a function of the internal structure (h_2), for PLATO, Kepler, JWST, and TESS.

Kepler, JWST and CHEOPS reach a $S/N > 3$, hence providing the means to constrain the internal structure of WASP-121b.

4. Summary and Conclusions

Close-in planets are subjected to high tidal and rotational surface deformations, leading to transit curve distortions. The magnitude of these distortions depend on the planetary internal structure, expressed through the Love numbers k_j (or equivalently h_j). We showed that PLATO, Kepler, JWST and CHEOPS have the means to constrain the second degree Love number of WASP-121b, providing additional invaluable information on its internal structure.

Acknowledgements

We acknowledge support from the DFG via the Research Unit FOR 2440 *Matter under planetary interior conditions*.

References

[1] Carter, J. A., and Winn, J.N.: Empirical constaints on the oblateness of an exoplanet, ApJ, 709:1219-1229, 2010.

[2] Correia, A.C.M.: Transit light curve and inner structure of close-in exoplanets, A&A, 570, L5, 2014.

[3] Kellermann, C., Becker, A., Redmer, R.: Interior structure models and fluid Love numbers of exoplanets in the super-Earth regime, A&A, accepted: February 2018.

[4] Kopal, Z.: Close binary systems, New York: Wiley, 1959

[5] Love, A.E.H.: Some problems of geodynamics, Cambridge University Press, 1911

[6] Sohl, F., Wagner, F.W., Rauer, H.: Mass-radius relationships of rocky exoplanets, Proceedings IAUS 293, 2012.

EPSC Abstracts
Vol. 12, EPSC2018-487, 2018
European Planetary Science Congress 2018

Light elements in planetary cores: a review

Guillaume Morard
Sorbonne Université, Muséum National d'Histoire Naturelle, UMR CNRS 7590, IRD, Institut de Minéralogie, de Physique des Matériaux et de Cosmochimie, IMPMC, 75005 Paris, France (guillaume.morard@upmc.fr)

Abstract

Planetary cores are mainly constituted of iron, however the presence of other elements could strongly affect its properties, such as melting temperature, liquid density and more generally phase diagrams. Each light elements commonly assessed, e.g. S, C, Si, O or H [1], must be considered individually, as their effects are highly different, and strongly depend on pressure, that is to say on the size of the planet considered. I will present here a review of the actual knowledge on light elements effects on iron properties, from the Moon's to exoplanets cores.

1. Introduction

From the nucleosynthesis sequence, iron is one the major non-volatile element during planetary accretion. Differentiation processes occurring for solar system planets extracted an iron-based core from a silicate-based mantle. Potential high pressure metal-silicate equilibration during magma ocean stage favors the presence of Si and O in planetary cores [2] (volatile-poor scenario), whereas the study of meteorites emphasize the presence of S and C in parent bodies of differentiated achondrites [3] (volatile-rich scenario).

However, each light elements would have strongly different impact on physical properties of the planetary core formed after the differentiation. On one hand, considering different types of mechanisms, volatile –rich or volatile-poor, the resulting properties of the planetary cores would be drastically different. On the other hand, integrated models of planetary interiors could help us to decipher what is the most probable core composition.

2. Experimental results

I will mainly discuss in this presentation Laser Heating Diamond Anvil Cell coupled with different diagnostics, such as diffraction, absorption, inelastic scattering but also chemical analysis of recovered samples. This global set of diagnostics for iron and iron alloys under high pressure and high temperature allows to have a large overview on how each light element affects the properties of iron, such as binary and ternary phase diagrams, but also density, sound velocity…

I will finally compare these results with ab initio calculations and dynamic compression experiments.

3. Implications for planetary cores

First, the hypothesis of a liquid outer core in the Moon constrains the presence of volatile elements, such as S or C, in its core. We recently proposed a structure for the Moon's core based on a recent dataset on Fe-S binary phase diagram [4], [5].

Secondly, the Earth's core composition derived from siderophile elements partitioning experiments imply the combined presence of Si and O in the Earth's core, from metal-silicate equilibrium [2]. However, present temperature at the Core-Mantle Boundary require the addition of volatile elements, such as C and S, to decrease metal crystallisation temperature [6].

Finally, binary and ternary phase diagrams will be discussed under extreme pressure, emphasizing the difference between different core composition and how it will affect the expected core properties, such as magnetic field generation.

Acknowledgements

This project have received funding from the European Research Council (ERC) under the European Union's Horizon 2020 research and innovation Programme (grant agreement No 670787)..

References

[1] J. P. Poirier, "Light elements in the Earth's outer core: A critical review," *Phys. Earth Planet. Inter.*, vol. 85, no. 3–4, pp. 319–337, 1994.

[2] J. Siebert, J. Badro, D. Antonangeli, and F. Ryerson, “Terrestrial Accretion Under Oxidising Conditions,” *Science (80-.).*, vol. 1194, no. March, 2013.

[3] N. L. Chabot, “Sulfur contents of the parental metallic cores of magmatic iron meteorites,” *Geochim. Cosmochim. Acta*, vol. 68, no. 17, pp. 3607–3618, 2004.

[4] D. Antonangeli, G. Morard, N. C. Schmerr, T. Komabayashi, M. Krisch, G. Fiquet, and Y. Fei, “Toward a mineral physics reference model for the Moon’s core.,” *Proc. Natl. Acad. Sci. U. S. A.*, vol. 112, no. 13, pp. 3916–9, 2015.

[5] G. Morard, G. Garbarino, D. Antonangeli, D. Andrault, N. Guignot, J. Siebert, M. Roberge, E. Boulard, A. Lincot, A. Denoeud, and S. Petitgirard, “Density measurements and structural properties of liquid and amorphous metals under high pressure,” *High Press. Res.*, vol. 34, no. 1, 2014.

[6] G. Morard, D. Andrault, D. Antonangeli, Y. Nakajima, A. L. Auzende, E. Boulard, S. Cervera, A. Clark, O. T. Lord, J. Siebert, V. Svitlyk, G. Garbarino, and M. Mezouar, “Fe – FeO and Fe – Fe 3 C melting relations at Earth ’ s core – mantle boundary conditions : Implications for a volatile-rich or oxygen-rich core,” *Earth Planet. Sci. Lett.*, vol. 473, pp. 94–103, 2017.

EPSC Abstracts
Vol. 12, EPSC2018-540, 2018
European Planetary Science Congress 2018

Ab-initio studies of ammonia-water mixtures at icy planet mantle conditions

Victor Naden Robinson (1), Miriam Marques (1), Jacob Christiansen (1), Yanchao Wang (2), Yanming Ma (2,3) and **Andreas Hermann** (1)
(1) Centre for Science at Extreme Conditions, School of Physics and Astronomy, The University of Edinburgh, Edinburgh, EH9 3FD, United Kingdom, (2) State Key Laboratory of Superhard Materials, College of Physics, Jilin University, Changchun 130012, China, (3) International Center for Future Science, Jilin University, Changchun 130012, China (a.hermann@ed.ac.uk)

Abstract

The interiors of icy planetary bodies contain large amounts of mixtures of the molecular ices of water, ammonia, and methane. To develop a detailed picture of these bodies' interiors it is crucial to understand how these compounds interact at extreme pressure and temperature conditions. We present here results combining electronic structure total energy calculations, crystal structure prediction methodology, and ab-initio molecular dynamics (MD), to study the phase evolution of ammonia-water mixtures under pressure. We show that ammonia-rich hydrates are preferred above 100 GPa, and discuss MD results on four different stoichiometric ammonia-water mixtures up to 500 GPa and 5000 K. We find the presence of superionic regions, where protons move freely in heavy nuclei lattices, analyse their diffusive properties and bond lifetimes, and establish their melting lines.

1. Introduction

Accurate models of the interior structure of planetary bodies, in our or other solar systems, are key to understanding their formation and many of their properties. For instance, the stratification (or lack thereof) of molecular mixtures inside icy planets' mantles influences their luminosity and cooling rates; and the presence (or not) of water stored inside rocky planets' mantles influences their convection rates, the magnitude of plate tectonics and presence of surface water. But direct measurements of planetary interiors are virtually impossible and laboratory experiments are difficult, which is why accurate computer simulations can make important contributions.

Amongst mixtures of planetary ices, ammonia-water compounds are arguably of the most chemical interest, because they can form fully connected $HOH \cdots NH_3$ and $H_2NH \cdots OH_2$ hydrogen bonded networks. Three stoichiometric mixtures exist in nature and close to ambient conditions: ammonia monohydrate (AMH, NH_3:H_2O=1:1), ammonia dihydrate (ADH, 1:2) and ammonia hemiydrate (AHH, 2:1). These mixtures have been studied experimentally up to 10's of GPa in pressure, and rich phase diagrams have been uncovered [1]. Computational studies have pushed individual mixtures to much higher pressures, to investigate their structural evolution and behaviour at elevated temperatures [2].

Here, we use density functional theory (DFT) to determine the electronic structure of a variety of stoichiometric ammonia-water binary mixtures, across a range of pressures up to 1 TPa, which enables us to compare their relative stability and trends in formation and decomposition under various conditions. We utilise the particle swarm optimisation method as implemented in the CALYPSO package [3] in conjunction with the CASTEP total energy software suite [4] to sample the crystalline configurational landscape and determine promising structural candidates for each stoichiometry at given pressure conditions.

These candidate structures form the basis to develop low-temperature phase diagrams of binary ammonia-water mixtures based on enthalpic relations, while MD calculations are used to probe the onset of superionicity and full melting in these compounds.

2. Results

While the cosmic abundance ratio of ammonia to water is roughly 1:7, we find that relative modest compression favours the formation of ammonia-*rich* hydrate compounds, in particular the 2:1 AHH phase [5]. In Figure 1 we summarise the results from a large set of crystal structure prediction runs at 300 GPa, by showing the relative formation enthalpies of a large set of stoichiometric binary mixtures. The convex hull of these data points (shown as the solid line) indicates all

stable phases. At 300 GPa, only a single ammonia-water mixture, AHH, should be stable against decomposition.

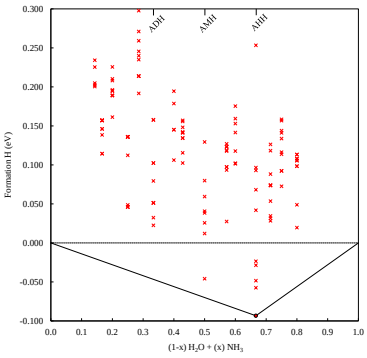

Figure 1: Convex hull construction of the formation enthalpies of the best ammonia-water mixtures found at 300 GPa.

We argue that this is due to energetically favourable de-protonation of water molecules under pressure, with the simultaneous formation of ammonium NH_4^+; this, in AHH, leads to the transformation from a hydrogen-bonded molecular mixture to a fully ionic compound. A dominant high-pressure phase of AHH has the archetypal CdI_2 ionic structure type, and is shown in Figure 2. The picture of different molecular entities is supported by a detailed analysis of the topologies of the eletronic charge density and the electron localisation function (ELF), which probes covalent bonding.

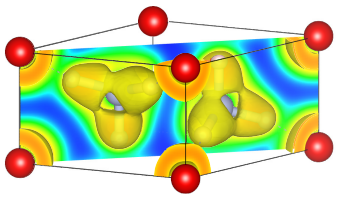

Figure 2: Electron localization function (ELF) isosurfaces and contours in the $P\bar{3}m1$ phase of AHH at 300 GPa, outlining the presence of isolated oxygen O^{2-} anions in a matrix of NH_4^+ cations.

The significant stabilisation of solid ionic structures under pressure has consequences for the high-pressure stability of ammonia-water mixtures – pushing the pressure of eventual decomposition into individual ices beyond 500 GPa – and the high-temperature behaviour of the mixtures: in ammonia-rich hydrates that support full de-protonation of water, the onset of superionicity (where protons become diffusive in a solid heavy ion lattice) is shifted to higher temperatures than in e.g. the 1:1 AMH compound. We will discuss the resulting P-T phase diagrams of the different relevant mixtures.

3. Summary

In this contribution we show that ammonia-water mixtures undergo a series of interesting phase transitions under pressure, leading to the stability of unusual ammonia-rich hydrates at pressures present inside the lower mantles of large icy planets. Their stabilisation is aided by the formation of ammonium oxides, and we present detailed analyses of the chemical bonding, vibrational properties, and high-temperature behaviour of the relevant phases.

Acknowledgements

V.N.R. and J.C. thank the EPSRC for funding through doctoral and career development studentships; M.M. thanks the ERC for funding. The authors gratefully acknowledge computing resources provided by the Royal Society, and by EPSRC through the UKCP consortium.

References

[1] Fortes, A. D. and Choukroun, M.: Phase behaviour of ices and hydrates. Space Sci. Rev., Vol. 153, pp. 185-218, 2010.

[2] Bethkenhagen, M., Cebulla, D., Redmer, R., and Hamel, S.: Superionic Phases of the 1:1 Water-Ammonia Mixture. J. Phys. Chem. A, Vol 119, pp. 10582-10588, 2015.

[3] Wang, Y., Lv, J., Zhu, L., and Ma, Y.: CALYPSO: A Method for Crystal Structure Prediction. Comput. Phys. Commun., Vol. 183, pp. 2063-2070, 2012.

[4] Clark, S. J., et al.: First Principles Methods using CASTEP. Z. Kristallogr., Vol. 220, pp. 567-570, 2005.

[5] Naden Robinson, V., Wang, Y., Ma, Y., and Hermann, A.: Stabilization of ammonia-rich hydrate inside icy planets. Proc. Natl. Acad. Sci., Vol. 114, pp. 9003-9008, 2017.

EPSC Abstracts
Vol. 12, EPSC2018-541, 2018
European Planetary Science Congress 2018

An experimental approach to investigate carbon rich exoplanets interior

Francesca Miozzi (1), Guillaume Morard (1) Daniele Antonangeli (1) Alisha N Clark (2) Caroline Dorn (3) Antoine Rozel (4) Mohamed Mezouar (5) Marzena A Baron (1) Anna Pakhomova (6) Guillaume Fiquet (1)

(1)Sorbonne Université, Muséum National d'Histoire Naturelle, UMR CNRS 7590, IRD, Institut de Minéralogie, de Physique des Matériaux et de Cosmochimie, IMPMC, 75005 Paris, France (francesca.miozzi@upmc.fr) (2) Department of Earth and Planetary Sciences, Northwestern University, Evanston, IL, USA, 60208. (3) University of Zurich, Institute of Computational Sciences, Winterthurerstrasse 109, CH-8057 Zurich. (4) Institute of Geophysics, Department of Earth Sciences, ETH Zurich, Sonneggstrasse 5, CH-8092 Zurich, Switzerland. (5) European Synchrotron Radiation Facility (ESRF). Grenoble, France. (6)Deutsches Elektronen-Synchrotron (DESY). Hamburg, Germany

Abstract

We experimentally determined properties (i.e. phase assemblage, thermal equation of state, melting temperature) of carbides (Si-C, Fe-Si-C) under extreme pressure and temperature conditions to constrain internal properties of carbon-rich exoplanets. By expanding the P-T-X range of these measurements, we can tightly constrain the phase diagram of binary and ternary carbide systems, and establish accurate P-V-T equation of state. Our experimental results are critically important for building reliable direct models for the interiors of exoplanets as well for interpreting observational data from recently launched survey missions such as TESS.

Introduction

An exciting recent development in space science has been the advancement of the exoplanet survey and the quest of an Earth's analog in other stellar systems. The launch of Kepler telescope in 2009 strongly contributed to the field, discovering more than a thousand exoplanets and for some also enabling to measure mass and radius. To further characterize those planets, the chemical composition can be inferred, though indirectly, by the elements distribution of the host star [1]. Knowledge of bulk composition and mineralogy of planetary interiors is central to understand their formation, present and past dynamics, including generation of magnetic field and surface processes, formation and sustainment of an atmosphere, all fundamental parameters to define the habitability of a planet.

Notably, some of the confirmed exoplanets have been observed orbiting around stars with an unusual chemical composition enriched in carbon instead of oxygen. This suggests that their mineralogical assemblages are potentially dominated by carbides instead of oxides. Carbon-rich planets are defined by a C/O ratio >0.8, and 55 Cancri e has been an archetype for this particular planets [2][3][4]. The TESS mission, with its scan range more than 20 times greater than Kepler, is likely to find also exoplanets orbiting around stars with exotic chemical composition. Accordingly, updated and diversified models are required for the interpretation of observational data.

Interiors of carbon-rich exoplanets were first modeled by computational methods using the mass and radius of 55 Cancri e as a reference [2]. The results of this study highlight how a mineralogy based on the Fe-Si-C system leads to multiple interior structures that all match the observed M/R. This clearly calls for an improved understanding of the properties of the Fe-Si-C system at relevant P-T conditions. Calculations by Wilson and Militzer [5] focused on the Si-C binary system up to 40 Mbar, and proposed possible planets interior made by SiC with different amount of C. In recent years further experimental studies on the Si-C system were published, however limited below 100 GPa [6]

In this contribution we will present experimental data collected on two different systems: 1) the binary Si-C and 2) the ternary Fe-Si-C, both investigated between 30 and 200 GPa and at temperatures up to 3300 K. The obtained results, provide insight on the stability and properties at high pressure of components that are candidates as constituent of carbon rich exoplanets.

Method

Experiments were performed at the European synchrotron radiation facility (ESRF) and at the Petra

III ring of the Deutsches Elektronen-Synchrotron (Desy), employing laser heated diamond anvil cells, coupled with *in-situ* x-ray diffraction. Samples were few micron thick layers of non-stoichiometric SiC and FeSiC sandwiched between KCl, used as a pressure medium, thermal insulator and pressure calibrant. Recovered samples were sectioned by FIB (focused ion beam) to expose the center of the heating spot, and chemical and textural analyses were performed by electron microscopy.

Results

The large amount of data collected on Si-C compounds allowed defining the exact P-T location and Clapeyron slope of the transition to the cubic rock salt structure, solving an on-going controversy. Furthermore the data collected for the high pressure structure were used to determine its thermal equation of state, still unknown, but of fundamental importance for the modelling of planetary interior. Finally, the phase diagram was examined, highlighting the strong dichotomy between the low melting temperature of the Si-rich side and the high melting temperature of the C-rich side, as well as the absence of intermediate compound between diamond and SiC (Miozzi et al., JGR Planets, under review). The Fe-Si-C ternary system has been probed using samples of different starting composition. Multiple eutectic melting curves were detected, together with changes in the phase assemblages and the solid liquid composition. The changes in the phase diagram affect the solid liquid composition and phase stability.

Application to Exoplanets Interiors

Two possible carbon rich exoplanets were modelled, both with SiC mantles and pure Fe cores. The first is a model of a planet with an iron core that make up for 1/3 of the mass. In the second model, the proportions of Fe and Si are chosen so as the bulk composition of the planet matches solar Fe/Si abundances. As shown in Figure 1, the first model yields to a mass-radius relationship very similar to the Earth-like planets. Thus there is a range of mass and radius for which is almost impossible to discriminate between and Earth-like interior or a carbon rich interior on the sole basis of the mass and radius.

This demonstrates the importance of having reliable models, coming from both computational and experimental studies, which can be used to interpret observational data for exoplanets.

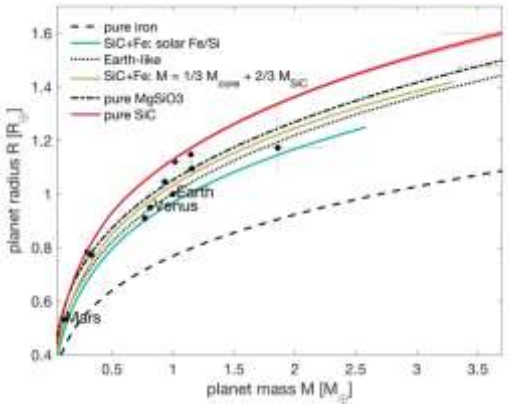

Figure 1: Mass radius relation for different idealized exoplanets interior, together with the standard comparison curves (e.g. pure Fe, $MgSiO_3$ and Earth-like).

Acknowledgements

This project and F.M., G. M. and G. F. have received funding from the European Research Council (ERC) under the European Union's Horizon 2020 research and innovation Programme (grant agreement No 670787). C.D. is funded by the Swiss National Science Foundation under the Ambizione grant PZ00P2_174028. A.B.R received founding from the European Research Council under the European Unions Seventh Framework Programme (FP/20072013)/ERC grant agreement number 320639 project iGEO and from ETH Zürich.

References

[1] Hinkel, Natalie, and Cayman Unterborn. 2017. "The Star-Planet Connection I: Using Stellar Composition to Observationally Constrain Planetary Mineralogy for the Ten Closest Stars.

[2] Madhusudhan, N., Lee, K. K. M. & Mousis, O. A POSSIBLE CARBON-RICH INTERIOR IN SUPER-EARTH 55 Cancri e. *Astrophys. J.* **759,** L40 (2012).

[3] Delgado Mena, E., Israelian, G., Gonzalez Hernandez, J. I., Bond, J. C., Santos, N. C., Udry, S. & Mayor, M. CHEMICAL CLUES ON THE FORMATION OF PLANETARY SYSTEMS : C / O VERSUS Mg / Si FOR HARPS GTO SAMPLE. 2349–2358 (2010). doi:10.1088/0004-637X/725/2/2349

[4] Teske, J. K., Cunha K, Smith V.V, Schuler S.C., & Griffith C.A. C/O Ratios of Stars with Transiting Hot Jupiter Exoplanets. Astrophysical Journal 788 (1) (2013).

[5] Wilson, H. F. & Militzer, B. Interior Phase Transformations and Mass-Radius Relationships of Silicon-Carbon Planets. *Astrophys. J.* **793,** 34 (2014).

[6] Kidokoro, Y., Umemoto, K., Hirose, K. & Ohishi, Y. Phase transition in SiC from zinc-blende to rock-salt structure and implications for carbon-rich extrasolar planets. *Am. Mineral.* **102,** 2230–2234 (2017).

EPSC Abstracts
Vol. 12, EPSC2018-558, 2018
European Planetary Science Congress 2018

Mantle mixing over time

Lena Noack and Alexander Balduin
Free University Berlin, Germany (lena.noack@fu-berlin.de)

Abstract

We evaluate under which conditions the ringwoodite-bridgmanite phase transition can separate Earth's mantle into two-layered convection and quantify the efficiency of material exchange between upper and lower mantle. Phase transitions and their Clapeyron slope depend on local composition (e.g. from primordial to depleted mantle material), temperature and pressure conditions [1].

1. Introduction

While Earth is a planet where for present-day processes in the interior and at the surface we have a wealth of information (with surface-mantle interactions as depicted in Fig. 1), data for the early evolution of the planet is sparse. Apart from few zircon inclusions that date back to Hadean times, first rock samples are limited to the end of the Eoarchaean and to the Archean time. These rock samples, while providing interesting single observations of early Earth's surface, are only some pieces of a much larger puzzle that we still need to solve to be able to explain why Earth developed to the unique habitable planet that we know.

Mantle temperatures have been estimated to exceed present-day temperatures by ~150-200 degree few Gyrs back into Earth's history [2], leading to the conclusion that the mantle may have been separated into two convecting layers [3], with few or no material exchange in-between (see Fig. 2). Such a layering would have strong implications for the thermal and chemical evolution of the upper and lower mantle, as well as for volatile cycles (if volatile recycling did exist on Hadean and Early Archaean Earth) from surface to the deep mantle. It is not clear, however, how strong the layering effect was in the past, and neither if a similar state would have occurred during Earth's earliest evolution after magma ocean solidification. It is therefore crucial to understand how changing temperature and pressure conditions for different Earth mantle compositions from primordial to depleted mantle may influence the Clapeyron slope of the ringwoodite-bridgmanite phase transition, and under which conditions and at which time (if at all) the mantle may have been separated into two mostly distinct layers.

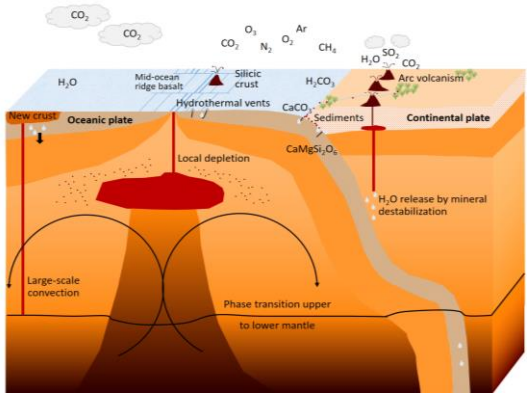

Figure 1: Sketch of Earth's present-day convective cycles from surface to interior. The depth profile of the sketch is logarithmic. [4]

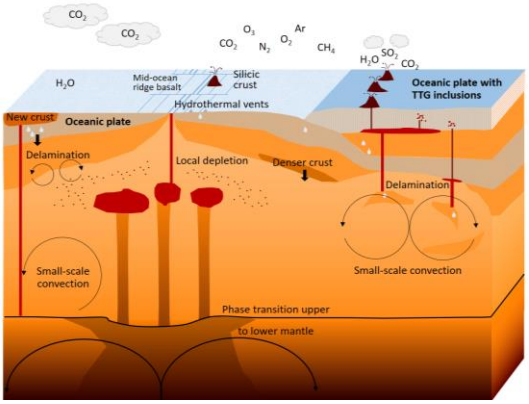

Figure 2: Sketch of possible Archaean's layered convection due to a hotter mantle. [4]

2. Model

The mantle convection code CHIC [5] solves the conservation equations of mass, momentum and energy in the compressible anelastic liquid approximation, to determine the mantle flow and thermo-chemical evolution of mantle rocks in a 2d spherical annulus. For all thermodynamic parameters (e.g. density ρ, thermal expansion coefficient α,

specific heat capacity c_p), local values depending on the local composition (based on the Mg-Fe-Si-O-Al-Ca-Na system [6]), temperature and pressure are used.

We apply different initial temperature profiles varying from adiabatic profiles based on the melting temperature of the mantle (end of magma ocean phase) to non-adiabatic profiles assuming a magma ocean overturn after the solidification stage [7,8].

3. Mineralogy and phase transitions

The Clapeyron slope, which determines the strength of the mineral phase transitions, is evaluated locally depending on the entropy and density (and therefore depending on composition, temperature and pressure).

$$\gamma \left[\frac{Pa}{K}\right] = \frac{S_2 - S_1}{V_2 - V_1} * Mmol = \frac{S_2 - S_1}{\frac{1}{\rho_2} - \frac{1}{\rho_1}}$$

We use Perple_X [9] to determine the phase stability fields for the major mineral phases occurring on Earth [1], which are used in CHIC to define the phase transition pressures of Earth's dominant minerals.

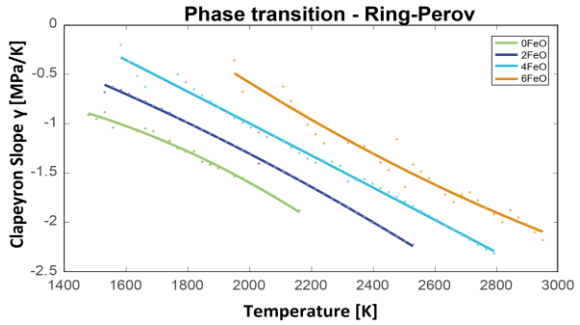

Figure 3: Clapeyron slope of the ringwoodite-bridgmanite phase transition depending on temperature and iron content calculated with Perple_X [9]. From [1].

EOS [6] are applied to obtain local information on thermodynamic properties for the mineral assemblage, including the Clapeyron slope (see Fig. 3) for accurate investigation of the influence of the phase transitions on the energy and momentum equation of the mantle. Figure 3 shows that the mantle composition (here looking at variable iron content based on pyrolite) strongly influences the strength of the Clapeyron slope. In addition, at lower temperatures, the negative Clapeyron slope is closer to zero, leading to a less strong effect on convective motion and temperature.

4. Summary and Conclusions

For a hotter (Archaean) Earth, the negative slope of the Clapeyron slope is larger, leading to a less efficient mixing between upper and lower mantle. In this study we quantify the effect of the ringwoodite-bridgmanite phase transition on mantle convection and mantle mixing. Changes in the convective style between two-layered and one-layered mantle convection can have global consequences due to a transition between heterogeneous mantle composition and efficient mixing consistent with the geological record [3].

References

[1] Balduin, A. and Noack, L.: Phase transitions in rocky mantles - influence of composition and temperature, EGU 2018, 8-13 April 2018, Vienna, Austria, 2018.

[2] Nisbet, E. G., Cheadle, M. J., Arndt, N. T. and Bickle, M. J.: Constraining the potential temperature of the Archaean mantle: a review of the evidence from komatiites, Lithos, 30(3-4):291-307, 1993.

[3] Breuer, D. and Spohn, T.: Possible flush instability in mantle convection at the Archaean–Proterozoic transition, Nature, 378(6557):608, 1995.

[4] Del Genio, A.D., and Brain, D., and Noack, L. and Schaefer, L.: The Inner Solar System's Habitability Through Time, in review.

[5] Noack, L., Rivoldini, A. and Van Hoolst, T.: Volcanism and outgassing of stagnant-lid planets: Implications for the habitable zone, PEPI, 269:40-57, 2017.

[6] Stixrude, L. and Lithgow-Bertelloni, C.: Thermodynamics of mantle minerals-II. Phase equilibria, GJI, 184(3):1180-1213, 2011.

[7] Elkins-Tanton, Linda T., Parmentier, E. M. and Hess P. C.: Magma ocean fractional crystallization and cumulate overturn in terrestrial planets: Implications for Mars, Meteoritics & Planetary Science, 38(12):1753-1771, 2003.

[8] Maurice, M., Tosi, N., Samuel, H., Plesa, A. C., Hüttig, C. and Breuer, D.: Onset of solid ‐ state mantle convection and mixing during magma ocean solidification, JGR: Planets, 122(3):577-598, 2017.

[9] Connolly, J. A. D: The geodynamic equation of state: what and how, G3, 10(10), 2009.

EPSC Abstracts
Vol. 12, EPSC2018-678-1, 2018
European Planetary Science Congress 2018

Effects of different equations of state on the interior structure of exoplanets

Philipp Baumeister (1), Jasmine MacKenzie (1), Nicola Tosi (1,2) and Mareike Godolt (1)
(1) Zentrum für Astronomie und Astrophysik, Technische Universität Berlin, Germany (philipp_baumeister@tu-berlin.de)
(2) Institut für Planetenforschung, Deutsches Zentrum für Luft- und Raumfahrt, Berlin, Germany

Abstract

In this work we aim at quantifying the influence of different isothermal and thermally-dependent equations of state (EoS) on the computation of the interior of exoplanets. We perform an extensive parameter study to model the interior structure of a vast number of sub-Neptunian exoplanets of different composition, ranging from super-Earths consisting just of a metallic core and a silicate mantle, to sub-Neptunes including ice and gaseous layers. Each model run is performed with a number of different isothermal as well as thermally-dependent EoS. We find that for the rocky interior of an exoplanet, the choice of EoS has little influence on the characterization of the interior structure of the planet.

1. Introduction

One of the major aspects of current exoplanetary science is the characterization of the planetary interior.

A common approach to characterize the interior of a known exoplanet is the use of numerical models to compute an interior structure which complies with the measured mass and radius of the planet [1, 2]. In general, however, possible solutions are highly degenerate, with multiple, qualitatively different interior compositions that can match the observations equally well (Fig. 1). It is therefore necessary to run numerous interior structure models covering a wide range of possible interior parameters to constrain solutions. In order to not increase any intrinsic degeneracy, it is also important to look at the impact of different parametrizations for both the interior and atmosphere combined. In this work we will mostly focus on the interior while keeping the atmosphere very simple.

The majority of computation time for an interior structure is spent solving the equations of state (EoS). For large parameter studies it is therefore beneficial to use the simplest EoS which still provide an accurate characterization of the planet's interior. In this work, we aim to investigate the differences in model interiors the use of different EoS entails.

2. Numerical Model

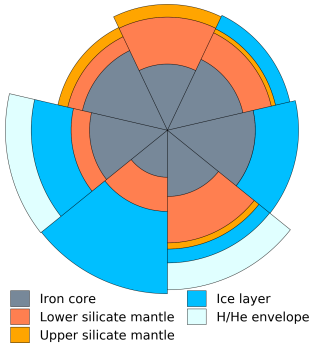

Figure 1: Seven interiors of an Earth-mass planet with varying core, ice and gas envelope mass fractions. The center top slice describes an Earth-like planet.

We employ a 1D structure model to construct sub-Neptunian exoplanets. A model planet consists of up to five layers: an iron-rich core, a lower silicate mantle composed of perovskite and magnesiowüstite, an upper silicate mantle composed of olivine and orthopyroxene, a potential water ice layer, and a gaseous envelope of varying composition (see Fig 1). The size of the core, the mantle as well as the ice layer are constrained by prescribed mass fractions. The interface between upper and lower mantle is defined by the plivine-perovskite phase transition at 23 GPa. We assume the interior to be convecting. The temperature then follows an adiabatic profile.

Each layer uses a prescribed equation of state to link pressure, temperature and density. We consider the following common formulations of EoS:

1. **3rd order Birch-Murnaghan [1, 3]:** This is a commonly used empirical EoS based on the finite

Eulerian strain. Temperature dependence is incorporated into the thermal expansion coefficient.

2. **Mie-Grüneisen-Debye [1, 3]:** In contrast to the Birch-Murnaghan EoS, the pressure is split into static pressure and thermal pressure terms. The thermal pressure is calculated based on the Debye model for specific heat. In the isothermal case, the Mie-Grüneisen-Debye EoS is equivalent to the isothermal Birch-Murnaghan EoS.
3. **Generalized Rydberg [4]:** This EoS is a generalization of the Vinet EoS [5], which is based on the interatomic repulsive potential. The thermal effect is incorporated as a pressure correction term, similar to the Mie-Grüneisen-Debye formulation.

The upper mantle uses the Birch-Murnaghan EoS. For the core, lower mantle and ice layer we utilize all EoS formulations described above. All models are tested with isothermal and thermally-dependent formulations.

For the moment, the gaseous envelope is modelled using a simple polytrope with polytropic index n=1.

We perform an extensive parameter study to assess the effect of different EoS on the observed radius of the modeled planet. Varied parameters are the planet mass, the mass fractions of each layer, the mantle potential temperature of the interior and the composition of the minerals constituting the material of the rocky layers.

3. Results

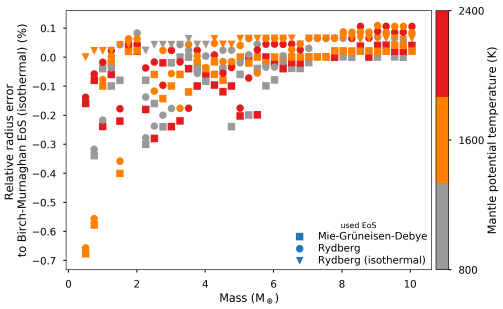

Figure 2: Relative radius errors of the EoS cases compared to the isothermal Birch-Murnaghan case for planet masses up to 10 $M_\oplus$ with a core-mass fraction of 0.3.

We find that in the case of an iron/silicate planet all EoS formulations result in computed planet radii which are less than 50 km apart in the most extreme case of a nearly molten planet. This amounts to a relative error of less than 0.7% in all cases studied (Fig. 2). This is an order of magnitude smaller than the precision we can expect for measurements of planetary radii in the near future (e.g. by the PLATO mission [6]). We conclude that for Earth-like planets the use of a simple isothermal EoS (in this case a 3rd order isothermal Birch-Murnaghan EoS) may be sufficient to accurately model the interior.

Acknowledgements

The authors acknowledge the support of the DFG priority program SPP 1992 "Exploring the Diversity of Extrasolar Planets (TO 704/3-1 & GO 2610/2-1)".

References

[1] Sotin, C., Grasset, O., and Mocquet, A. (2007). Mass-radius curve for extrasolar Earth-like planets and ocean planets. Icarus 191.

[2] Seager, S. et al. (2007). Mass-Radius Relationships for Solid Exoplanets. ApJ 669.

[3] Jackson, I. (1998) Elasticity, composition and temperature of the Earth's lower mantle: A reappraisal. Geophys. J. Int. 134.

[4] Wagner, F.W. et al. (2012). Rocky super-Earth interiors Structure and internal dynamics of CoRoT-7b and Kepler-10b. Astronomy and Astrophysics 541.

[5] Stacey, F.D. (2005). High pressure equations of state and planetary interiors. Rep. Prog. Phys. 68.

[6] Rauer, H. et al. (2014). The PLATO 2.0 mission. Experimental Astronomy 38.

EPSC Abstracts
Vol. 12, EPSC2018-684, 2018
European Planetary Science Congress 2018

Fluid Love numbers with the matrix propagator method with an application to GJ436b

Sebastiano Padovan, Doris Breuer, Szilard Csizmadia, Hugo Hellard, Heike Rauer, Frank Sohl, and Tilman Spohn
Institute of Planetary Research, German Aerospace Center (DLR), Berlin, Germany (sebastiano.padovan@dlr.de)

Abstract

Investigations of the interior structure of exoplanets mostly rely on their measured radius and mass. Large observational errors and the intrinsic non-uniqueness of mass-radius relationships limit the inferences that can be made. The expected future determination of the fluid Love number k_2, which is sensitive to the interior structure, provides an additional constraint. We illustrate here an analytical method to calculate the fluid Love numbers based on the matrix propagator method, and apply it to the object GJ436b. We show that a precise measurement of its k_2 might partially solve some of the current degeneracies present in mass-radius relationships.

1. Introduction

The ever-blooming catalogue of exoplanets counts more than 3700 confirmed members (e.g., https://exoplanetarchive.ipac.caltech.edu). For about 10% of these objects a reliable mass M and radius R have been measured and the resulting bulk density provides a first handle on the interior structure—e.g., rocky vs. gaseous. However, a given M-R pair can be compatible with different interior structures as in the case of GJ436b [1]. The fluid Love number k_2, which depends on the concentration of mass in the interior similarly to the moment of inertia, can provide an additional constraint. Its determination can be obtained through photometry and/or measurement of the orbital precession. With improving instruments and continuous observations, the number of exoplanets for which M, R, and k_2 will be available will steadily increase.

2. Fluid Love numbers with the matrix propagator method

The calculation of the Love numbers can be obtained from the solution of the equation (e.g., [2])

$$T_{\mathrm{n}}''(r)+\frac{2}{r}T_{\mathrm{n}}'+\left[\frac{4\pi G\rho'(r)}{V'(r)}-\frac{n(n+1)}{r^2}\right]T_n(r)=0, \tag{1}$$

where r, V, and ρ are the radial coordinate, the gravitational potential, and the density of the unperturbed body (i.e., spherically symmetric), respectively. A prime indicates derivation with respect to r, and $V'(r) = -g(r)$ the gravitational acceleration. The function T has the dimensions of a potential and describes the total change in potential of the planet under a perturbing potential (e.g., tidal potential, rotational potential). Mixed boundary conditions are applied at the center ($r = 0$), where T must be finite, and at at the surface ($r = R_{\mathrm{P}}$), where its derivative must be continuous. It can be shown (e.g., [2]), that the fluid Love numbers k_n and h_n can be obtained from

$$k_{\mathrm{n}}=\frac{T_{\mathrm{n}}(R_{\mathrm{P}})}{R_{\mathrm{P}}g(R_{\mathrm{P}})}-1, \quad h_{\mathrm{n}}=k_{\mathrm{n}}+1 \tag{2}$$

where the subscript n indicates the degree in the harmonic expansion of the perturbing potential.

The solution of equation (1) with mixed boundary conditions can be obtained with the shooting method (e.g., [4]). Alternatively, by discretising the internal density profile of a given interior model, the term dependent on the radial density derivative in equation (1) can be dropped and the equation reduces to an Euler-Cauchy equation, which we solve with the matrix propagator method (e.g., [5]). We recast the second-order differential equation as a system of two first-order equations in the non-dimensional quantities $\mathbf{y}_1$ and $\mathbf{y}_2$, defined as

$$T = \frac{GM}{R}\mathbf{y}_1, \tag{3}$$

$$P = \frac{dT}{dr}=\frac{GM}{R^2}\left(\frac{R}{r}\right)\mathbf{y}_2. \tag{4}$$

By adopting power solutions for the $\mathbf{y}$'s and imposing continuity of T and P across internal boundaries–i.e., at each density jump–it is possible to obtain the solution for $\mathbf{y}$ at the surface and, through equations (2) and (3), to determine the value of k_{n}.

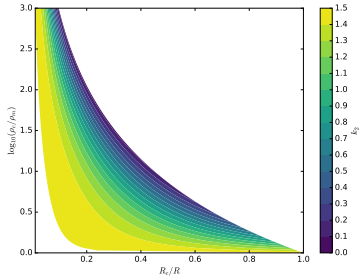

Figure 1: For a two constant-density layer model, fluid Love number k_2 (colors) as a function of the radius of the core and the density contrast ρ_c/ρ_m.

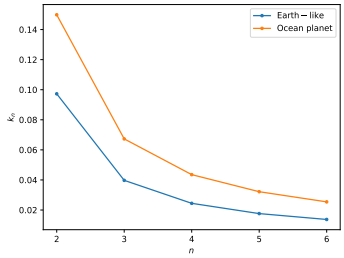

Figure 2: Value of k_n as a function of n for two different interior models of GJ436b, an Earth-like model and an Ocean-planet model (described in [1]).

3. Results

3.1. Interior structure and k_2

We use a two constant-density layer planet model to illustrate the relation between the Love number k_2 and mass concentration in the planet. The parameters of the model are the core density ρ_c, the mantle density ρ_m, the radius of the core R_C, and the radius R. Figure 1 shows how k_2 varies as a function of the radius of the core and the density contrast between core and mantle. In the case of equal density in the core and mantle, or of a very small core, k_2 reaches the value of 1.5, characteristics of a homogeneous body. For the opposite case of a small high-density core, k_2 approaches the value of 0, which corresponds to a point-mass core surrounded by a massless envelope. Intermediate values indicate various concentration of mass in the interior.

3.2. Application to GJ436b

As an application we choose the planet GJ436b, a roughly 21 Earth masses and 4.3 Earth radii planet. We apply the matrix propagator method to two possible interior models [1], an Earth-like model with a very dense metallic core surrounded by a silicate mantle, and a water rich model with a silicate core and a water mantle. Both models have an outer hydrogen/helium envelope and are compatible with the measured mass and radius. We digitised the density profiles published in [1] and computed the fluid Love number k_n for n = 2,3,4,5,6. The results are shown in Figure 2. The Earth-like model, characterised by a dense core, which corresponds to a more concentrated density profile, has a smaller value for the k_n considered.

4. Summary and Conclusions

We developed a python package, which we intend to freely release, to compute the fluid Love numbers k_n and h_n for a given interior structure model using the matrix propagator method. The accurate knowledge of M, R, and k_n cannot remove the degeneracy present in interior structure models comprising more than two layers [3], but may allow to broadly discriminate the interior model classes, e.g., Earth-like versus Ocean-planet for the case GJ436b as illustrated in Figure 2.

Acknowledgements

This work was supported by the DFG within the Research Unit FOR 2440 "Matter Under Planetary Interior Conditions".

References

[1] Adams, E.R., et al.: Ocean planet or thick atmosphere: on the mass-radius relationship for solid exoplanets with massive atmosphere, ApJ, Vol. 673, pp. 1160-1164, 2008.

[2] Gavrilov, S.V., et al.: Influence of tides on the gravitational field of Jupiter, Sov. Astron., Vol 19, 618-621.

[3] Kramm, U., et al.: On the degeneracy of the tidal Love number k_2 in multi-layer planetary models: application to Saturn and GJ436b, A&A, Vol. 528, A18, 2011.

[4] Press, W.H., et al.: Numerical Recipes 3rd Edition: The Art of Scientific Computing, Cambridge Univ. Press, 2007.

[5] Wolf, D: Lamé's problem of gravitational viscoelasticity, Geophys. J. Int., Vol 116, 321-348.

EPSC Abstracts
Vol. 12, EPSC2018-858, 2018
European Planetary Science Congress 2018

Interior structure of WASP-18b through its apsidal motion

Szilárd Csizmadia, Hugo Hellard and Alexis M. S. Smith
DLR, Institute of Planetary Research, 12489 Berlin, Rutherfordtrstr 2., Germany (szilard.csizmadia@dlr.de)

Abstract

Exoplanets and their host stars exhibit a mutual tidal interaction. One of the consequences of this phenomenon is the so-called apsidal motion: the major axis of the eccentric orbits rotate around the host star and it is called either apsidal motion or periastron precession. The rate of this precession linearly depends on the k_2 fluiud Love-number of the planet and therefore this effect, when this motion is observable, provides an opportunity to measure it. Theoretical predictions suggest that WASP-18b is one of the systems which features the biggest apsidal motion rate which should be observable by radial velocities and by transit timing variations within a few years. We analyze the available archival radial velocity data and we are able to give an upper limit for its Love-number.

1. Introduction

Increasing our knowledge of the interior structure, composition and density distribution of exoplanets is crucial to make progress in the understanding of formation, migration, habitability etc. of exoplanets. However, the directly-measurable mass and radius values offer little constraint on interior structure, because the problem is highly degenerate. Therefore there is a clear need for a third observable of exoplanet interiors: the Love-number that is a measure of internal density distribution of planets.

Tidal interactions between exoplanets and their host stars can be much stronger than experienced in our own Solar System. This is because exoplanets may have much shorter orbital periods and smaller orbital distances than Mercury (88 days). Many exoplanets have an orbital period less than 10 days which increases the efficiency of the star-planet interaction.

The consequences of tidal interaction in close-in systems are – among others – change in the semi-major axis (tidal decay) on a time-scale of billions years, change in the eccentricity in hundreds of millions of years (circularization), change in the rotational rate (synchronization) in tens of millions of years and precession of the major axis of the orbit around the star (apsidal motion) which occurs on the time scale of years to decades [1].

Since a few exoplanets were already discovered ten-twenty years ago it is valuable and feasible to search for this kind of apsidal motion and to utilize it in planet interior studies.

2. Theoretical background

Periastron precession consists of a general relativistic term (GR) and a classical, Newtonian term (N):

$$\dot{\omega} = \dot{\omega}_N + \dot{\omega}_{GR}$$

The GR term is:

$$\dot{\omega_{GR}} = \frac{6\pi G M_{star}}{a c^2 (1-e^2)}$$

while the tidal-term (Newtonian-term) is

$$\dot{\omega}_N = \frac{n}{2} \Sigma_{i=1}^{2} \left(\frac{R_i}{a} \right)^5 k_{2,i} F(P_i, P_{orb}, M_{planet}, M_{star}, e)$$

where we used the usual notation (G is the gravitational constant, M are the masses, c is the speed of the light, n is the mean motion, a is the semi-major axis, R is the radius, e is the eccentricity, Ps are the rotational and orbital periods).

The apsidal motion is reflected in the measured radial velocities because its zero point is calculated from the periastron point that precesses.

In Figure 1 we show the magnitude of the change in argument of periastron over 10 years (i.e. $\Delta\omega = 10\ years \times \dot{\omega}$). Notice that we assumed $k_2 = 0.4$ for the Jupiter-sized exoplanets and $k_2 = 0.8$ for the superearths.

Presently, the most accurate measurements are able to obtain the value of omega with 2-3 degrees. Considering this value and Figure 1, we feel we are able to measure k_2 from the periastron precesison.

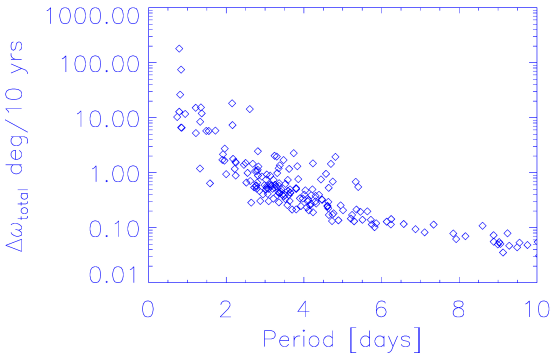

Figure 1: Orbital period vs expected periastron precession rate for exoplanets. Eccentricity and other values were taken from www.exoplanet.eu. Notice the logarithmic scale on y-axis. Exoplanets below 1 day orbital period gives chance to measure this apsidal motion and to determine the Love-number of some exoplanets.

3. WASP-18b

WASP-18b has an orbital period of only 0.94 days, a mass of 10.4 Jupiter-mass and a radius of 1.17 Jupiter-radii. The eccentricity is small, ~0.01, but significant and confirmed by the Spitzer Space Telescope [2]. Therefore it is an ideal target for such studies.

We collected all archival radial velocity measurements and modelled them [3,4,5,6]. Our preliminary result is that

$$\dot{\omega} = 0.008 \pm 0.003\, degree/day.$$

This yields approximately $k_2 < 0.50$, a value not far from Jupiter's value ($k_2 \sim 0.4$) in our own Solar System.

We submitted proposals to get telescope time in order to obtain a more precise value and to confirm our previous, preliminary findings.

4. Outlook

We started a work to measure the k_2 fluid Love-number of close-in exoplanets via the apsidal motion of them. We utilize archival and new data for this unique work.

New results can be expected between the submission of the abstract and the presentation of this work during EPSC. With this method we can present a few upper limits as well as precisely measured Love-number values which are fundamental for planetary interior studies.

Acknowledgements

We acknowledge support from the DFG via the Research Unit FOR 2440 Matter under planetary interior conditions and from the DFG German Priority Program SPP 1992 'Mass-radius diversity of exoplanets'.

References

[1] Iorio, L.: Classical and relativistic long-term time variations of some observables for transiting exoplanets, MNRAS 411, pp. 167-183, 2011

[2] Bonomo, A. S. et al.: The GAPS Programme with HARPS-N at TNG . XIV. Investigating giant planet migration history via improved eccentricity and mass determination for 231 transiting planets, A&A 602, A107, 2017

[3] Albrecht, S., et al.: Obliquities of Hot Jupiter Host Stars: Evidence for Tidal Interactions and Primordial Misalignments 2012, ApJ 757, 18

[4] Knutson, H. A., et al.: Friends of Hot Jupiters. I. A Radial Velocity Search for Massive, Long-period Companions to Close-in Gas Giant Planets2014, ApJ 785, 126

[5] Esposito, M., et al.,: The GAPS Programme with HARPS-N at TNG. A&A 601, A53

[6] Hellier, C., et al.: An orbital period of 0.94days for the hot-Jupiter planet WASP-18b 2009, Nature 460, 1098

EPSC Abstracts
Vol. 12, EPSC2018-1195, 2018
European Planetary Science Congress 2018

Jupiter internal structure: the role of the equations of state

Yamila Miguel (1) and Tristan Guillot (2)
(1)Leiden Observatory, Netherlands (2)Observatoire de la Cote dÁzur, France (ymiguel@strw.leidenuniv.nl)

Abstract

A better knowledge of Jupiter's atmosphere and internal structure is key to understand the formation and evolution of the biggest giant of the solar system.

Juno mission is orbiting Jupiter since July 2016 and its highly accurate gravity measurements [1, 2, 3] are causing a revolution in our knowledge of the planetary interior and atmosphere, leading to a much better comprehension of the big giant [4, 5, 6].

We use this outstanding gravity data to perform models of Jupiter's internal structure and test different parameters to get a better understanding of Jupiter's interior. Our results show that the accuracy of interior model calculations still relies on the determination of the properties of hydrogen and helium at high pressures [7, 8, 9, 10]. In this talk I am going to show the effect of different equations of state in Jupiter internal structure and in the determination on its differential rotation.

References

[1] Bolton, S., et al.: Jupiter's interior and deep atmosphere: The initial pole-to-pole passes with the Juno spacecraft, Science, Vol. 356, pp. 821-825, 2017.

[2] Folkner, W. M. et al.: Jupiter gravity field estimated from the first two Juno orbits, Geophys. Res. Lett., Vol 44, 4694-4700, 2017.

[3] Iess, L. et al.: Measurement of Jupiter's asymmetric gravity field, Nature, Vol 555, pp. 220-222, 2018.

[4] Wahl, S. M. et al.: Comparing Jupiter interior structure models to Juno gravity measurements and the role of an expanded core: Geophys. Res. Lett., Vol 44, pp. 4649-4659, 2017.

[5] Guillot, T., Miguel, Y., et al.: A suppression of differential rotation in Jupiter's deep interior, Nature, Vol 555, pp. 227-230, 2018.

[6] Kaspi, Y. et al.: Jupiter's atmospheric jet streams extend thousands of kilometres deep, Nature, Vol 555, pp. 223-226, 2018.

[7] Saumon, D., and Guillot, T.: Shock Compression of Deuterium and the Interiors of Jupiter and Saturn, ApJ, Vol. 609, pp. 1170-1180, 2004

[8] Fortney, J. And Nettelmann, N.: The Interior Structure, Composition, and Evolution of Giant Planets, Space Science Reviews, Vol. 152, pp. 423-447, 2010

[9] Baraffe, I., Chabrier, G., Fortney, J., and Sotin, C.: Planetary Internal Structures, Protostars and Planets VI, Henrik Beuther, Ralf S. Klessen, Cornelis P. Dullemond, and Thomas Henning (eds.), University of Arizona Press, Tucson, 914 pp., p.763-786, 2014

[10] Miguel, Y., Guillot, T., and Fayon, L.: Jupiter internal structure: the effect of different equations of state, A&A, Vol 596, 12 pp., 2016

EPSC Abstracts
Vol. 12, EPSC2018-1235, 2018
European Planetary Science Congress 2018

Miscibility gap of hydrogen-helium mixtures

Manuel Schöttler, Ronald Redmer
Institut für Physik, Universität Rostock, Germany

Abstract

We calculate the high-pressure demixing phase diagram of hydrogen-helium mixtures [1], which is important for applications in planetary physics, in particular, for calculating the interior and evolution of gas giants. The separation of hydrogen and helium has long been proposed as a possible source of Saturn's excess luminosity: The initially hot planet cools down with increasing age and when the planetary isentrope intersects with the demixing region [2], helium-rich droplets can form and sink toward the planetary core, thus, acting as an additional source of heat; see, e.g., [3].

The region of demixing is observed from thermodynamic relations by computing the free enthalpy G(x,P,T) at constant pressure P and temperature T for different helium fractions x. We use finite-temperature density functional theory molecular dynamic simulations to obtain the equation of state for given volumes and temperatures. The non-ideal entropy of mixing is calculated using a combination of coupling-constant integration and thermodynamic integration of the equation of state.

The choice of an appropriate exchange-correlation (XC) functional is of paramount importance. It has been shown that standard approximations such as PBE lack the ability to adequately describe the metallization transition in hydrogen [4], which is directly connected to the H-He demixing. Functionals that take into account non-local correlations such as vdW-DF [5] are in better agreement with recent experiments [4]. Benchmarking studies with many XC functionals against QMC calculations suggest vdW-DF as an appropriate functional also for hydrogen-helium mixtures [6].

Here, we present a demixing phase diagram of H-He mixtures calculated with vdW-DF and compare with previous calculations derived with the PBE functional [7, 8]. Differences and implications for planetary physics are discussed, in particular, for the gas giants Jupiter and Saturn.

References

[1] Schöttler and Redmer, PRL 120, 115703 (2018)

[2] Stevenson, PRB 12, 3999 (1975)

[3] Püstow et al., Icarus 267, 323 (2016).

[4] Knudson et al., Science 348, 1455 (2015).

[5] Dion et al., PRL 92, 246401 (2004).

[6] Clay et al., PRB 89, 184106 (2014).

[7] Lorenzen et al., PRL 102, 115701 (2009).

[8] Morales et al., PRB 87, 174105 (2013).